Chemosphere 313 (2023) 137519

Contents lists available at ScienceDirect

Chemosphere

journal homepage: www.elsevier.com/locate/chemosphere

Embryotoxicity and visual-motor response of functionalized nanostructured hydroxyapatite-based biomaterials in zebrafish (*Danio rerio*)

Augusto Monteiro de Souza [a], Heloysa Araujo-Silva [b], Andréa Machado Costa [c], Andre Linhares Rossi [c], Alexandre Malta Rossi [c], José Mauro Granjeiro [d], Ana Carolina Luchiari [b], Silvia Regina Batistuzzo de Medeiros [a,*]

[a] Department of Cell Biology and Genetics, Biosciences Center, Federal University of Rio Grande do Norte, Natal, RN, Brazil
[b] Department of Physiology & Behavior, Federal University of Rio Grande do Norte, Natal, RN, Brazil
[c] Department of Condensed Matter, Applied Physics and Nanoscience, Brazilian Center for Physics Research, Rio de Janeiro, Rio de Janeiro, Brazil
[d] Directory of Life Sciences Applied Metrology, National Institute of Metrology, Quality and Technology, Duque de Caxias, Rio de Janeiro, Brazil

HIGHLIGHTS

- Functionalized hydroxyapatite-based nanomaterials were characterized by electron transmission microscopy (TEM).
- The embryotoxicity test showed no effect of Hydroxyapatite-based microspheres.
- There were no changes in the development of embryos exposed to different biomaterials.
- The behavioral test showed no neurotoxicity.
- HA-based microspheres show biosecurity and should be used in bone regeneration.

GRAPHICAL ABSTRACT

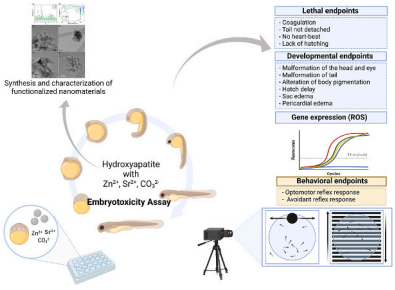

ARTICLE INFO

Handling Editor: James Lazorchak

Keywords:
Zebrafish embryotoxicity test
Developmental toxicity
Hydroxyapatite microspheres
Visual-motor behavior

ABSTRACT

Hydroxyapatite (HA) is a biomaterial widely used in biomedical applications. Many studies have shown that ionic substituents can be incorporated into HA to produce a mineral composition more similar to natural bone tissue with more favorable biological characteristics for application in bone regeneration. However, its potentially toxic effects need to be evaluated before full approval for human use. For this purpose, an embryotoxicity test was performed on zebrafish according to OECD guideline 236. Zebrafish embryos were exposed to 1 or 3 microspheres of alginate containing nanoparticles of HA and carbonate (CHA), strontium (SrHA), and zinc-substituted HA (ZnHA) from 4 to 120 h post-fertilization (hpf). Lethality and developmental endpoints were evaluated. In addition, larval behavior at 168 hpf was also analyzed to observe whether biomaterials adversely affect optomotor and avoidance responses (neurotoxicity), as well as the oxidative stress pattern through qPCR. After 120 h exposure to all microspheres with different patterns of crystallinity, porosity, nanoparticle size, surface area, and degradation behavior, there was no mortality rate greater than 20%, indicating the non-embryotoxic character of these biomaterials. All experimental groups showed positive optomotor and

* Corresponding author. Department of Cellular Biology and Genetics, Bioscience Center, Federal University of Rio Grande do Norte, Campus Universitário, Natal, RN CEP 59072, Brazil.
E-mail address: silvia.batistuzzo@ufrn.br (S.R. Batistuzzo de Medeiros).

https://doi.org/10.1016/j.chemosphere.2022.137519
Received 17 September 2022; Received in revised form 29 November 2022; Accepted 7 December 2022
Available online 8 December 2022

avoidance responses, which means that embryo exposure to the tested biomaterials had no neurotoxic effects. Furthermore, larvae exposed to one SrHA microsphere showed a better optomotor response than the control. Furthermore, the biomaterials did not change the pattern of mRNA levels of genes related to oxidative stress even after 120 hpf. The growing number of new HA-based biomaterials produced should be accompanied by increased studies to understand the biosafety of these compounds, especially in alternative models, such as zebrafish embryos. These results reinforce our hypothesis that ion-substituted HA biomaterials do not impose toxicological effects, cause development and neuromotor impairment, or increase oxidative stress in zebrafish embryos being useful for medical devices and in the process of bone regeneration.

1. Introduction

With the increasing biotechnological advances in recent decades, areas such as cell biology, molecular biology, and the development of nano and micro biomaterials have resulted in a significant increase in the production and evaluation of new devices for medical and pharmaceutical applications (Melchor-Martínez et al., 2021). While these new biomaterials have promising and unique properties, there are growing concerns that these new properties could also make them toxic, resulting in potential risks to human health.

The risk of toxicity may develop when a biomaterial is implanted in the human body. An excellent biomaterial, not toxic and widely used for implants is calcium phosphate ceramic based on Hydroxyapatite (HA). It is usually used as a bone filler or a coating for implants because it allows greater fixation of the implant to the bone tissue. Indeed, bone tissue is a nanocomposite consisting of a collagenous matrix and carbonated hydroxyapatite (CHA) nanocrystals, with a needle or plate-like shape, with dimensions of 20–80 nm in length and 2–5 nm in thickness. HA, chemical formula ($Ca_{10}(PO_4)_6(OH)_2$), is the main mineral composing human hard tissues (bones and teeth) (Ratnayake et al., 2016). Therefore, due to their excellent biocompatibility, HA-based biomaterials, functionalized or not, have been widely studied for application in several areas, especially in bone tissue engineering (Ghorbani et al., 2015; Sari et al., 2021; Wang et al., 2014). The ionic substitution of HA-based biomaterials offers an outstanding option to modify the physicochemical structure of HA by adding ions that change the properties of these biomaterials, such as mechanical properties, biocompatibility, bone adhesion, and osteogenic stimulation properties.

Despite their application in several areas, there are opposing opinions about the potential of HA-based biomaterials, as their functionalization may present different physicochemical properties. Many studies in vitro and in vivo have reported that HA is non-toxic for biomedical applications, with these biomaterials being a promising alternative for bone regeneration (Coelho et al., 2019; Melchior et al., 2018; Remya et al., 2017). On the contrary, some studies report that HA may produce toxicity and inflammation in the body tissues and even genotoxicity (Morscher et al., 1998; Mosa et al., 2020; Turkez et al., 2014). For instance, axial column deformations were observed in zebrafish larvae exposed to HAp NP (Zhao et al., 2013).

The use of zebrafish (*Danio rerio*) as an alternative model is fundamental to establishing the safety of a product, currently being more widely used in research studies for ontogenetic development, pharmacology, toxicology, and translational neuroscience (Xu et al., 2012). Zebrafish Information Network (ZFIN) (https://zfin.org/) is a database of genetic and genomic data for zebrafish and presents it as a model organism due to the following characteristics: 1) great ease of research; 2) high genetic similarity with the human genome, 70% gene homology); 3) the fast and efficient time to obtain quality results; and 4) the existence of well-established protocols in the Organization for Economic Co-operation and Development (OECD). Such characteristics were crucial for the choice of zebrafish to observe the effects of nanostructured HA-based biomaterials during its development. In this context, this study aimed to evaluate the acute toxicity responses of HA-based nanoparticles with different ionic substitutions (Zn^{2+}, Sr^{2+}, CO_3^{2+}) in zebrafish embryos to understand its effects on development and behavior since monitoring of embryos in the presence of these biomaterials is important for the successful use of the compounds in the bone regeneration process. We hypothesize that transient developmental exposure from 4 to 168 h post-fertilization (hpf) in zebrafish embryos to functionalized HA-based nanostructured biomaterials present no toxic, developmental, or behavioral effect over time.

2. Materials and methods

2.1. Synthesis and preparation of microspheres from HA-based biomaterials

Hydroxyapatite nanoparticles were synthesized by the wet method. An aqueous solution of $(NH4)_2HPO_4$ was dropwise to an aqueous solution of $Ca(NO_3)\cdot 4H_2O$. The pH was kept at ten by adding KOH, and after 03 h, the precipitate was separated by filtration and repeatedly washed with cold water; all reagents were Merck p.a. grade. The material was lyophilized, and the dried powder was manually ground. Particles <210 μm were separated by sieving (Supplementary Table 1).

Cation-substituted hydroxyapatite was prepared with 5% of Ca^{2+} sites substituted by Zn^{2+} or Sr^{2+} ions. Briefly, solutions of $Ca(NO_3)\cdot 4H_2O$ and $Zn(NO_3)_2$ (or $Sr(NO_3)_2$) were dropwise by a peristaltic pump to an aqueous solution of $(NH_4)_2HPO_4$. The pH was kept at nine by the addition of KOH. After 03 h, the precipitate was separated by filtration and repeatedly washed with cold water; all reagents were Merck P.A. grade (Terra et al., 2002). The suspension was lyophilized, and the dried powder was manually ground. Particles <210 μm were separated by sieving (Supplementary Table 1).

For the preparation of anion-substituted hydroxyapatite nanoparticles, 6% of PO_4^{3-} sites were substituted by CO_3^{2-} ions on the HA structure. Then, an aqueous solution of $Ca(NO_3)_2\cdot 4H_2O$ was dropwise in a reactor containing $(NH_4)HPO_4$ and $(NH_4)_2CO_3$; the mixture was kept at pH 9–10 using NH_4OH for 03 h. All reagents were Merck P.A. The materials were filtered and washed with milli-Q water, and the powders were crushed and sieved at 210 μm (Terra et al., 2009) (Supplementary Table 1).

A dispersion of the nanoparticles produced alginate microspheres containing HA or ion-substituted HA nanoparticles with 10 mg/mL aqueous solution of sodium alginate (Fluka Biochemika, Buchs, Switzerland) to achieve a 1:15 alginate-HA ratio. The alginate/HA mixture was extruded dropwise at room temperature into a 0.15 M $CaCl_2$ solution using a needle with a 0.70 mm diameter (BD Precision Glide, Sao Paulo, SP, Brazil). Spherical particles were instantaneously formed and were left in the $CaCl_2$ solution for 24 h for complete gelation. The HA-alginate microspheres were dried overnight at 30 °C and sieved to obtain microspheres with diameters of 425–600 μm.

2.2. Materials characterization

The Ca, Zn, and Sr contents of the HA, CHA, ZnHA, and SrHA nanoparticles were determined by quantitative chemical analysis after acid treatment with HNO_3. The obtained solutions were diluted and analyzed using atomic absorption spectroscopy (AAS) using a Shimadzu 6800 instrument. The phosphate content was obtained by vanadomolybdate phosphoric acid colorimetric method, using a UV–Vis

spectrophotometry (Shimadzu UV-2450) at 420 nm. Carbon content was evaluated by using a triplicate of CHA samples that were calcined at 1350 °C in an oxygen atmosphere where they underwent an oxy-reduction process. In the end, the carbon present in both samples was converted to CO_2; the quantification was obtained using an SC-144DR Sulfur and Carbon Analyzer.

The crystallographic phases, lattice parameters, and crystalline order were analyzed on the D-8 Advance Brucker diffractometer with Cu-Kα radiation (λ = 1.54 Å) at 40 kV and 40 mA. Diffraction patterns were collected from 2θ b 20°–40° in a step of 0.02° at 5s/step. XRD peaks at 25.8° and 32.9° related to the diffraction 002 and 300 hkl planes, respectively, were fitted by Lorentzian curves to obtain half width using the software Origin 7.0 program and the crystallite means size in directions c (D002) and a (D300) were determinate by Scherrer Equation (1): Dhkl = 0.89 λ/βcos ((2θ)/2), (1) λ = wavelength Cu radiation (1.54 Å), β = half width of the peak relative to hkl plane (radians), 2θ = diffraction angle (radians). Fourier transform infrared spectroscopy (FTIR) was used to detect the vibration modes of CHA, and the spectra were collected using a Perkin Elmer Spectrum One spectrophotometer over a range of 4000–400 cm−1 at a resolution of 2 cm−1 and 128 scans using KBr pellets. The specific surface area of all powder samples and microspheres was determined by measurements using a Micro metrics 3 Flex operating in the N_2 physisorption technique in the 8-point BET method after a pre-treatment at 200 °C/1 h for degassing.

The morphology of HA, CHA, ZnHA, and SrHA nanoparticles was characterized by Transmission Electron Microscopy (TEM) using a JEOL 2100F equipment operated at 200 kV of accelerating voltage. Images were acquired with an ONEVIEW 16 MP digital camera.

2.3. Animals and housing

The Animal Ethics Committee approved this study at the Federal University of Rio Grande do Norte (CEUA 33.060/2018). All experiments with zebrafish were performed at the Fish Lab in the Department of Physiology and Behavior at the Federal University of Rio Grande do Norte.

Adult zebrafish (*Danio rerio*, WT strain, four months, female/male 2:3, 0.400 ± 0.300 g) were purchased from a local farm (Natal-RN, Brazil) and kept in the Fish Lab of the Federal University of Rio Grande do Norte. We used an outbreed population due to larger genetic variability between individuals that resembles the variability of the general human population. The fish were maintained in an automated rack system (ZebTEC Active Blue Stand Alone - Tecniplast®) under a light-dark cycle of 14–10 h for at least three months before breeding. Fish were kept at a density of 2–3 animals per liter in unenriched acrylic tanks and water-controlled conditions: 28 °C; pH 7.2; total ammonia at <0.01 mg/L; and conductivity of 1,600 μS/cm. The fish were fed with brine shrimp *Artemia* sp. (*Artemia salina* do RN®, Brazil), and commercial flake food (Alcon Basic®, Brazil; 60% protein and 15% fat). Food was offered three times daily. These fish compose the stock population.

2.4. Obtaining embryos

For breeding, adult fish were selected by chance and placed in breeding tanks in a proportion of three females to two males. Breeding tanks were filled with system water and maintained in the same conditions described above. On the following day, eggs were collected around 60 min after the lights turned on. Viable eggs, identified by blastula formation at 3 h post-fertilization (hpf) were separated, washed with system water, and transferred to 24-well polystyrene plates (1 embryo/well).

2.5. Acute toxicity test

The animal number proposed in the present study was based on the guidelines and protocols established by the "Fish Embryo Acute Toxicity (FET)" (OECD 236). Each well was filled with 1 mL of system water with one or three microspheres of each biomaterial (mean mass of microspheres: 80 μg for blank, SrHA, and ZnHA; 120 μg for HA and 90 μg for CHA). One microsphere was used to test the lowest mass of biomaterials produced, while 3 microspheres were applied in an attempt to overload the embryo kinetics, which depends on the number of chemicals available. We also included positive (4 mg/L of 3,4-dichloroaniline) and negative (rack system water) controls. Four embryos were used as internal plate controls.

Embryos were exposed to the biomaterials for 120 h. Every 24 h the embryos were observed under a stereomicroscope at 80× magnification to verify lethality signs: egg clotting, absence of somite formation, tail base non-displacement, heartbeat lack, pericardial edema occurrence, yolk sac edema, eye edema, body pigmentation alterations, as also malformation of head, sacculi/otoliths, tail, heart, and spinal cord structure modified.

2.6. Behavioral analysis

Larvae with 7dpf previously treated with the biomaterials described above were exposed to two moving stimuli to measure optomotor and avoidance responses, following the methodology described by Creton (2009). Both stimuli were applied using a PowerPoint projection on a computer screen, where a Petri dish (8.5 cm diameter) with larvae was sited. All behavioral tests were performed between 10 a.m. and 12 p.m. to avoid influencing animals' locomotor activities and visual sensitivity. Behavioral analyses were performed in duplicates to one microsphere (n = 18 larvae per group), and three microspheres (n = 15 larvae per group).

The first test to evaluate the optomotor response was a pattern of moving stripes consisting of alternating black and white stripes (24.5 cm × 1.5 cm; Fig. 1a). First, the stripes moved up for 1min with an interval of 5s without any stimulus (white screen). Following the interval, the stripes moved down for another 1min. The moving stripes stimuli were repeated 10 times at a constant speed (1 cm/s), and the video recorded larvae behavior. At the end of each minute, when the blank background has been presented, subjects cognitively able to follow the stripe movements were considered positively fit. In contrast, those who did not follow the stripe patterns were identified with a negative optomotor response.

The second stimulus to assess the avoidance response consisted of a black circle "bouncing ball" (2.5 cm diameter) alternating between left and right movements (Fig. 1b). The test evaluated whether the larva was on the same side of the Petri dish on which the black circle was moving or if it showed avoidance behavior. To standardize, the black circle evermore moved in a straight line on the lower half of the plate, covering 10 cm trajectories in 3s (3.3 cm/s). The aversive behavior of the larvae was evaluated during 10 min of filming, and 40 images were analyzed when the bouncing ball was adjacent to the culture plate (on the right side of the dish). Images were imported into ImageJ (http://rsb.info.nih.gov/ij/index.html) to obtain larval orientation compared to the centroid. Larvae were identified and the X and Y coordinates were exported to Microsoft Excel. The coordinates obtained were standardized according to the centroid value.

2.7. RNA extraction and quantitative real-time polymerase chain reaction

Twenty zebrafish embryos of up to 3 hpf were exposed to one/three microspheres of the different biomaterials, 120 hpf of the larvae were sacrificed on ice, and the total RNA of the larvae was extracted and reverse transcribed for quantitative real-time polymerase chain reaction (qPCR). For extraction and isolation, the PuriLink RNA Mini Kit (Life Technologies) used all instructions were followed in full as stated in the manufacturer's protocol. After the end of the extraction, the total RNA was quantified in a NanoDropTM One Microvolume UV–Vis Spectrophotometer with a purity ratio between 1.8 and 2.0. Quality was

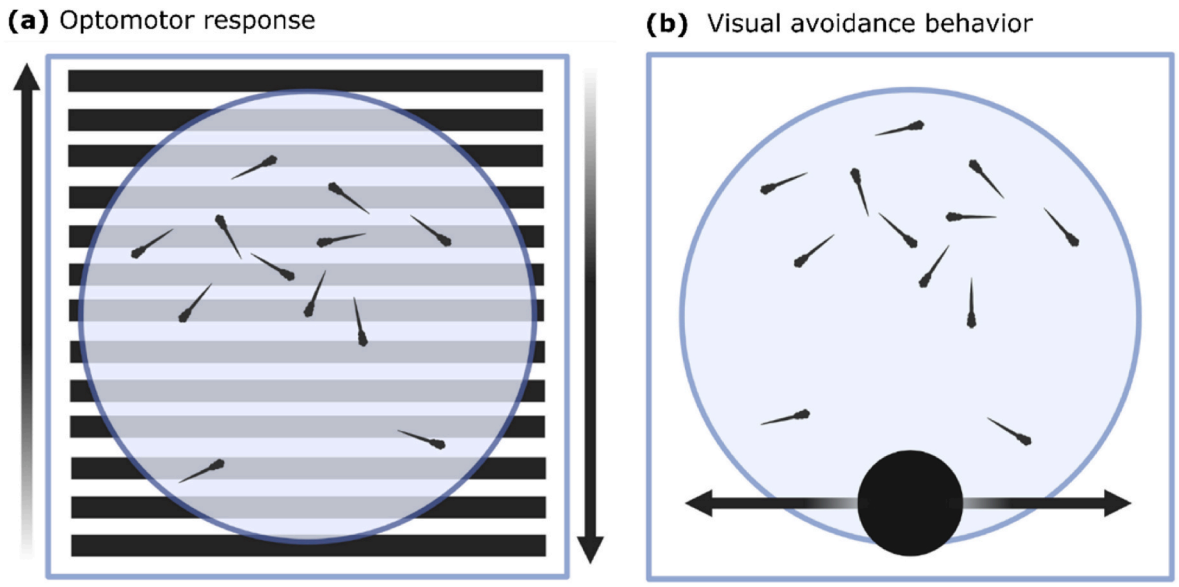

Fig. 1. Visual-motor behavioral analysis of zebrafish. Zebrafish larvae at seven dpf were filmed in the vertical configuration on a culture plate (8.5 cm in diameter) as described by Creton (2009). **(a)** Optomotor response, stripes moved at a constant upward velocity for 1 min and downward velocity for 1 min, 10 times. **(b)** Avoidance response, the black ball alternates from left to right in the lower half of the culture dish for 10 min.

determined by 0.8% agarose gel electrophoresis. All groups were standardized at a concentration of 100 ng/μL and stored in a freezer at −80 °C. The high-throughput cDNA reverse transcription kit (Applied Biosystems) was used to construct the cDNA. In this process, a mixture containing 10X RT buffer, 25X dNTP Mix, 10X RT Randon Primer, Reverse Transcriptase, and Nuclease-Free-Water was placed together with the RNA from the samples, at a concentration of 1 μg/μL.

The qPCR reactions were performed with the PowerUp SYBR® Green Master Mix (Thermo Fisher Science, Waltham, MA, USA) using the Rotor-gene Q system (Qiagen, CA, USA). We analyzed the relative expression levels ($^{2-\Delta\Delta Ct}$ fold change) of four genes associated with oxidative stress (superoxide dismutase 1 (sod1), superoxide dismutase 2 (sod2), catalase (cat), glutathione peroxidase 1A (gpx1a)), listed in Supplementary Table 2. Relative mRNA expression was quantified using the $^{2-\Delta\Delta Ct}$ method with β-actin as an endogenous control. The experiment was performed in triplicate and two independent replicates, following the Minimum Information Guidelines for Publication of Quantitative Real-Time PCR Experiments (MIQE) (Bustin et al., 2009).

2.8. Statistical analysis

Statistical analysis was conducted in the R program (R-Studio version 4.0.1 for windows). Data normality and homoscedasticity were tested using Shapiro-Wilk and Levene tests, respectively. Data presenting non-parametric distribution were compared by the Kruskal-Wallis test. A comparison of survival curves was performed using the log-rank (Mantel-Cox) test. For malformation analysis, we performed a Two-Way ANOVA considering factors "malformations" and "groups" followed by Dunnett's post hoc test to compare groups to the negative control. For optomotor response, the chi-square test was used to determine if groups followed the stripe movements. Linear Mixed Models (LMM) and post hoc Bonferroni tests were used to evaluate the interaction between X and Y coordinates, considering them as a dependent quantitative variable. Treatments and photos were considered fixed effect variables, and observation was a random effect variable. The evaluation of oxidative stress gene expression was performed by one-way analysis of variance (ANOVA) followed by Bonferroni's post hoc test. Data were analyzed using "tidyverse'', "rstatix'', "ggpubr'' and "emmeans" packages (Kassambara, 2020a, 2020b; Lenth and Lenth, 2018; Wickham et al., 2019). We considered an alpha level of 0.05 for statistical significance.

3. Results

3.1. Physicochemical analysis and characterization

The amount of Sr, Zn, and CO_3^{2-} in SrHA, ZnHA, and CHA powders is shown in Table 1. The Ca/P molar ratio of HA and SrHA samples was close to the stoichiometric value (Ca/P = 1.67) while ZnHA had a lower Ca/P molar ratio. The XRD patterns of HA, CHA, ZnHA, and SrHA powders were indexed using a hydroxyapatite pattern file ((JCPDS no. 09–0432, hexagonal crystal system, space group of P63/m); no crystalline secondary phases were detected (Fig. 2a). FTIR spectra of HA, CHA, ZnHA, and SrHA powders had similar profiles with characteristics bands of O–H at 3570 cm^{-1} and 632 cm^{-1}, phosphates at 1095 cm^{-1}, 1034 cm^{-1}, 960 cm^{-1}, 602 $cm^{-1,}$ and 565 cm^{-1}, carbonates at 1455 cm^{-1} and 1420 cm^{-1} and water at 3440 and 1640 cm^{-1}, (Fig. 2b) (Venkateswarlu et al., 2014; Wang et al., 2010).

The crystalline order determined by XRD for all samples along and perpendicular to the c axis (crystallite dimensions) is characteristic of elongating nanocrystals (Table 1). Electron transmission microscopy (TEM) analyses show that HA, CHA, ZnHA, and SrHA nanoparticles form agglomerates with sizes up to 700 nm (Fig. 2c–f). HA and ZnHA particles have needle-shaped, with 70–110 nm in length and 10–20 nm in thickness, (Fig. 2c and e, respectively), whereas SrHA was plate-shaped, with 20–40 nm in length and 7–10 nm in thickness (Fig. 2f). CHA is constituted of spheroid nanoparticles with average sizes of 50 nm (Fig. 2d). The high Ca/P molar ratio of the CHA sample (Ca/P > 1.67) confirmed the partial substitution of carbonate species in PO_4^{3-} sites. A

Table 1
Physicochemical characterization of HA and partially substituted-HA samples. Ca/P molar rate, Zn, Sr and Carbonate content, BET surface area, and crystallite dimensions.

Sample	Ca/P (Molar ratio)	CO_3 % Mass	%M/(M + Ca)	Area	D_{300}	D_{002}	300/002
HA	1.63	–	–	83	14.8	24.7	1.668
ZnHA	1.55	–	5.3	170	5.57	15.5	2.782
SrHA	1.69	–	3.8	65.5	16.1	38.8	2.409
CHA	1.794	0.8	–	72.4	13.8	28.9	2.094

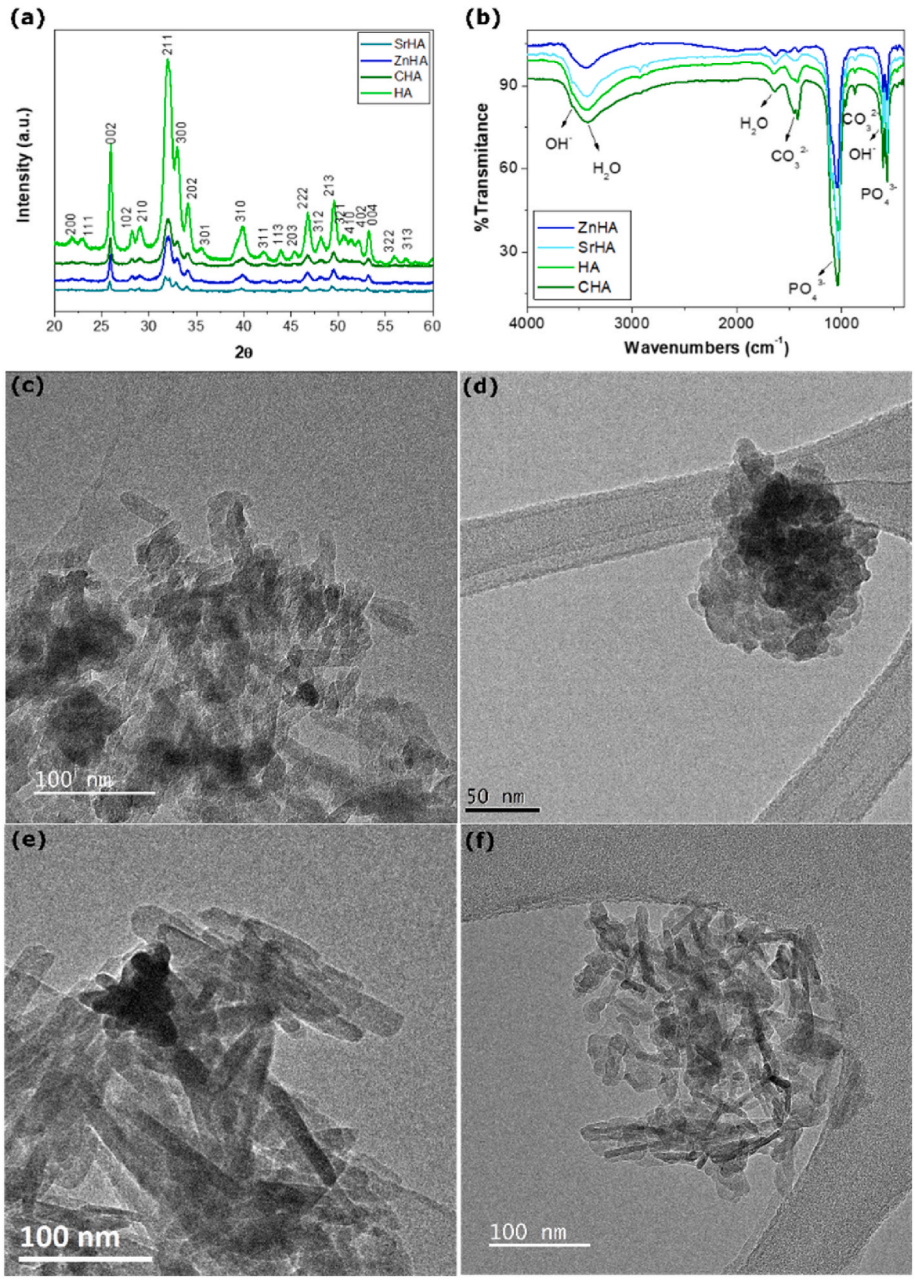

Fig. 2. Ion-substituted HA characterization: **(a)** XRD patterns of HA, CHA, ZnHA, and SrHA samples, **(b)** FTIR spectra of HA, CHA, ZnHA, and SrHA samples. Electron transmission microscopy (TEM) images of agglomerates of HA **(c)**, CHA **(d)**, ZnHA **(e),** and SrHA **(f)** nanoparticles.

higher specific surface area and a smaller size crystal was found for ZnHA nanoparticles compared with CHA and SrHA ones.

3.2. Lethal endpoints

During 120 h of experiment with one microsphere, the negative control presented 93.3% survival. For the positive control group, the survival rate was 23.3%. For the biomaterial-treated fish, the survival rate of zebrafish was 96.6% for White and HA, 95% for CHA, 98.3% for SrHA, and 88.3% for ZnHA groups (Fig. 3a). Despite survival rate variation in total number, the log-rank test showed statistical significance to positive control concerning the other groups ($\chi^2 = 614.7$, $p < 0.0001$). For three microspheres, the negative control presented 83.3% survival. The positive control group survival rate was 16.6%. For the biomaterial-treated fish, the survival rate was 93.3% for HA, 88.3% for White, CHA, and SrHA, and 80% for ZnHA (Fig. 3b). The log-rank test showed statistical significance to positive control regarding the other groups ($\chi^2 = 439.9$, $p < 0.0001$).

3.3. Developmental endpoints

Our results show that embryos treated with one or three microspheres showed no morphological defects. Two-way ANOVA revealed a statistically significant effect for groups (One microsphere: $F_{(6,\ 126)} = 64.54$, $p < 0.0001$; three microspheres: $F_{(6,\ 126)} = 112.38$, $p < 0.0001$), for malformations (One microsphere: $F_{(8,\ 126)} = 7.55$, $p < 0.0001$; three microspheres: $F_{(8,\ 126)} = 29.75$, $p < 0.0001$), and for the interaction terms (One microsphere: $F_{(48,\ 126)} = 6.63$, $p < 0.0001$; three microspheres: $F_{(48,\ 126)} = 14.21$, $p < 0.0001$). Dunnett's test showed that only fish exposed to positive control presented phenotypic abnormalities (Fig. 4, $p < 0.05$).

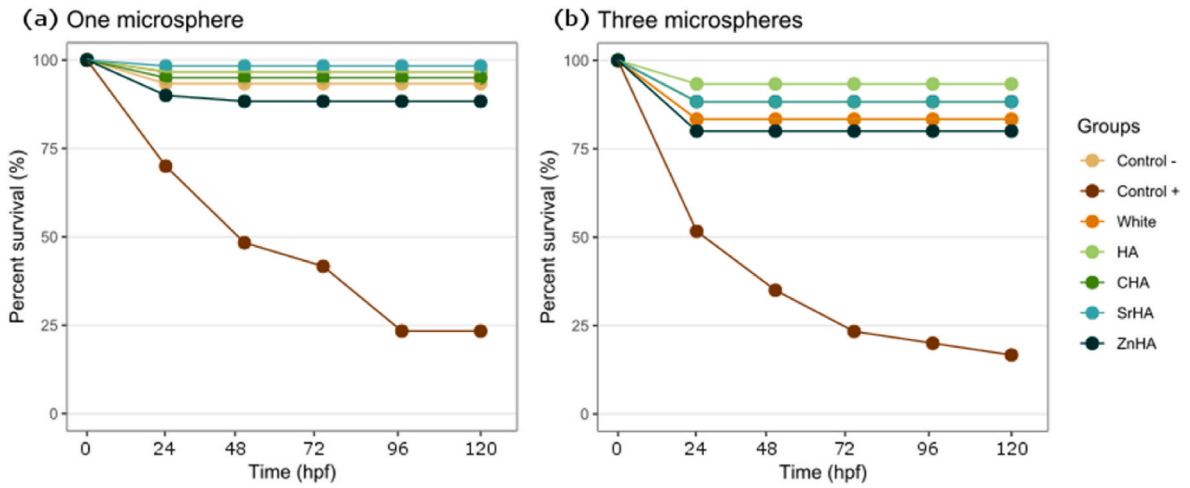

Fig. 3. Zebrafish survival curve with **(a)** one microsphere and **(b)** three microspheres. Fish were exposed to 7 treatments for 120 h: Control -, Control +, White, HA, CHA, SrHA, and ZnHA, and mortality was checked every day (inicial n = 60 per group).

3.4. Behavioral endpoints

Larvae optomotor response was registered and compared between treatments at 7dpf. Kruskal Wallis analysis showed no statistical significance between groups of one microsphere ($H = 7.98$, $df = 5$, $p = 0.15$; Fig. 5a) or three microspheres ($H = 10.5$, $df = 5$, $p = 0.06$; Fig. 5b). The proportion of fish that followed the stripe movement was significantly different between groups ($\chi^2 = 17.7$, $df = 5$, $p = 0.003$; Fig. 5c) of one microsphere. Pairwise comparison showed that during the larval experiment, the proportion of the White group differed from SrHA. For three microspheres the proportion of fish did not differ ($\chi^2 = 3.94$, $df = 5$, $p = 0.55$; Fig. 5d).

The avoidance response is presented in Fig. 6. To evaluate the interaction between X and Y coordinates we performed an LMM. For treatments with one microsphere, there was no significant difference for the X coordinate. LMM did not show significative effects for groups ($\chi^2 = 5.53$, $df = 5$, $p = 0.37$; Fig. 6a), photos ($\chi^2 = 2.36$, $df = 1$, $p = 0.12$; Fig. 6a) or interaction between groups × photo ($\chi^2 = 5.21$, $df = 5$, $p = 0.39$; Fig. 6a). For the Y coordinate, LMM found significative effects for groups ($\chi^2 = 50.49$, $df = 5$, $p < 0.0001$; Fig. 6a), and interaction groups × photos ($\chi^2 = 19.99$, $df = 5$, $p = 0.001$; Fig. 6a), but no effect for photos ($\chi^2 = 0.28$, $df = 1$, $p = 0.59$; Fig. 6a). The Bonferroni post hoc test showed a difference between groups HA and CHA along the Y coordinate ($p < 0.05$). For treatments with three microspheres, there was a significant difference for the X coordinate. LMM found significative effects for groups ($\chi^2 = 10.98$, $df = 5$, $p = 0.05$; Fig. 6b), photos ($\chi^2 = 20.30$, $df = 1$, $p < 0.0001$; Fig. 6b), and interaction terms groups × photo ($\chi^2 = 19.07$, $df = 5$, $p = 0.001$; Fig. 6b). The Bonferroni post hoc test showed the difference between Control and HA, CHA, and ZnHA ($p < 0.05$). For the Y coordinate, LMM found significative effects for groups ($\chi^2 = 68.80$, $df = 5$, $p < 0.0001$; Fig. 6b), photos ($\chi^2 = 3.89$, $df = 1$, $p = 0.04$; Fig. 6b), and interaction groups × photos ($\chi^2 = 63.63$, $df = 5$, $p < 0.0001$; Fig. 6b). The post hoc test showed a difference between CHA, Control, and ZnHA (Bonferroni: $p < 0.05$).

3.5. Oxidative stress genes expression

As the biomaterials did not significantly affect the development of zebrafish embryos/larvae, we evaluated whether there were molecular changes in the mRNA levels of genes involved in antioxidant defense in larvae after 120hpf exposure (Supplementary Figs. 1a and 1b). One-way analysis of variance (ANOVA) followed by Bonferroni's post hoc test did not show a significant change in superoxide dismutase 1 (sod1) mRNA levels in all biomaterials, under both conditions (One and Three microspheres), ($F(10, 11) = 1.517$; $p = 0.2521$). Concerning superoxide dismutase 2 (sod2), no changes were observed in the levels of transcripts of this gene, among all groups, compared to the expression of this gene in the negative control ($F(10, 11) = 0.9025$; $p = 0$ 0.5604). Regarding the mRNA levels of catalase (cat), and glutathione peroxidase 1 A (gpx1a) One-way ANOVA also revealed no statistical significance between groups, for both one ($F(10, 11) = 0.5757$; $p = 0.8034$) and three ($F(10, 11) = 0.6288$; $p = 0.7635$) microspheres compared to the negative control.

4. Discussion

This study contributed to understanding the toxicological responses of functionalized HA-based materials used in the bone regeneration process. We prepared a nanostructured HA-based bioactive alginate microsphere containing HA nanoparticles with and without carbonate ions, zinc, and strontium substitutions, and here we present the physicochemical characteristics and the toxicity results obtained in embryotoxicity assay.

The HA-based biomaterials in this study have different physicochemical properties, such as crystallinity, nanoparticle size, and specific surface area. However, these particularities did not significantly affect the toxic potential, exposing relatively similar profiles to the negative control.

Most studies suggest that a smaller particle size creates a larger specific surface area, resulting in higher bioavailability or surface activity of the particles. In turn, this can lead to increased toxicity. (Ferdous and Nemmar, 2020; Lin et al., 2013). In this context, there was slight toxicity, although not significant, for ZnHA nanoparticles concerning SrHA and CHA, which can be explained by the fact that this biomaterial has a higher specific surface area due to the smaller size of the crystals in addition to the shape-needle, factors that contribute to a slight increase in toxic effects.

In the last 20 years at PubChem (https://pubchem.ncbi.nlm.nih.gov/) more than 4014 patents have been filed for HA-based related biomaterials, which can be used for applications such as bone tissue engineering, bone cavity filling for orthopedics and traumatology, desensitizing agent in post-tooth whitening, remineralizing agent in toothpaste, drug, and gene delivery, among other applications (Cao et al., 2020; Dewi and Ana, 2018; Mohan et al., 2018; Subramaniam et al., 2016). The wide use of HA-based biomaterials in several areas derives from its advantageous properties, such as its excellent biocompatibility in addition to the bioactive properties that allow HA to interact with bone tissue more easily. The development of nanostructured

Fig. 4. Several phenotypic abnormalities were observed during 120 h of zebrafish development for all treatments with **(a)** one microsphere and **(b)** three microspheres. Two-way ANOVA followed by Dunnett's test was performed. Asterisks indicate statistical significance among groups (n = 60 per group, $p < 0.05$).

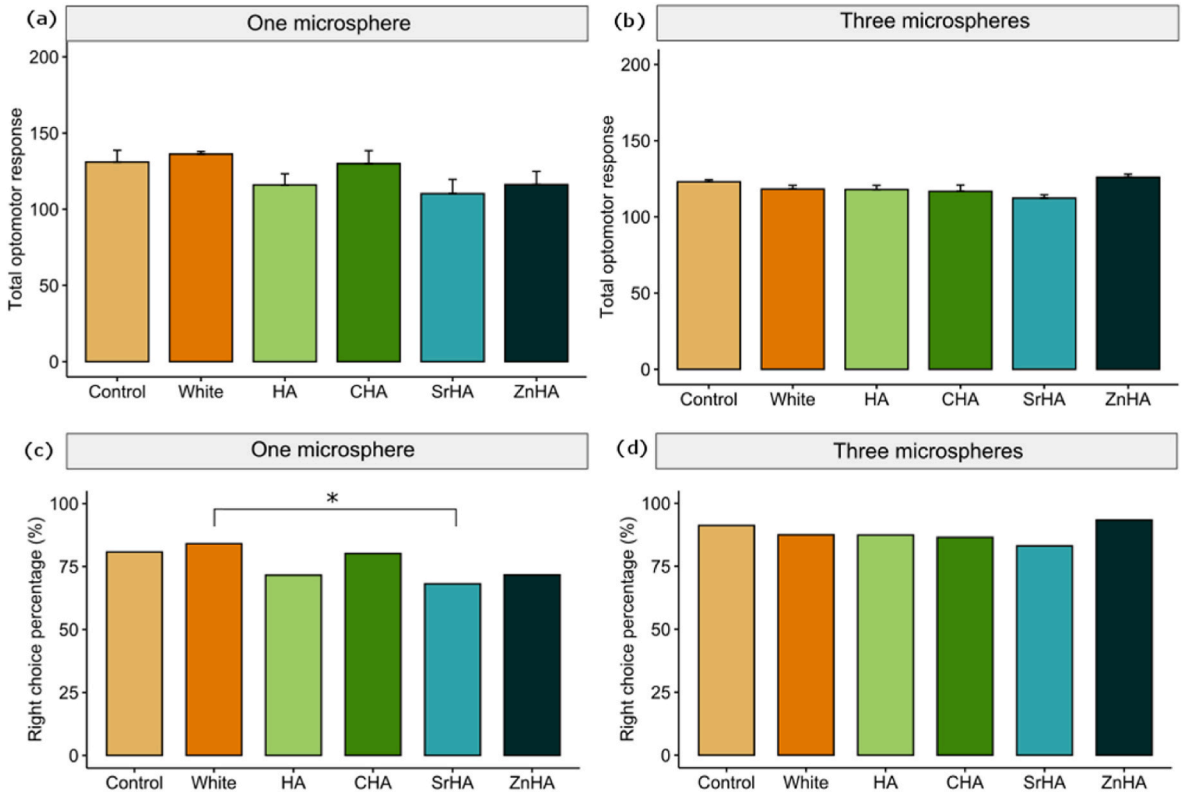

Fig. 5. Total larval optomotor responses (7dpf) following band movement after 120 h treatment with **(a)** one microsphere and **(b)** three microspheres, bars represent mean ± SEM. Percentage of correct answers (positive optomotor response) **(c)** one microsphere and **(d)** three microspheres of HA-based biomaterials. (Kruskal Wallis test, $p > 0.05$).

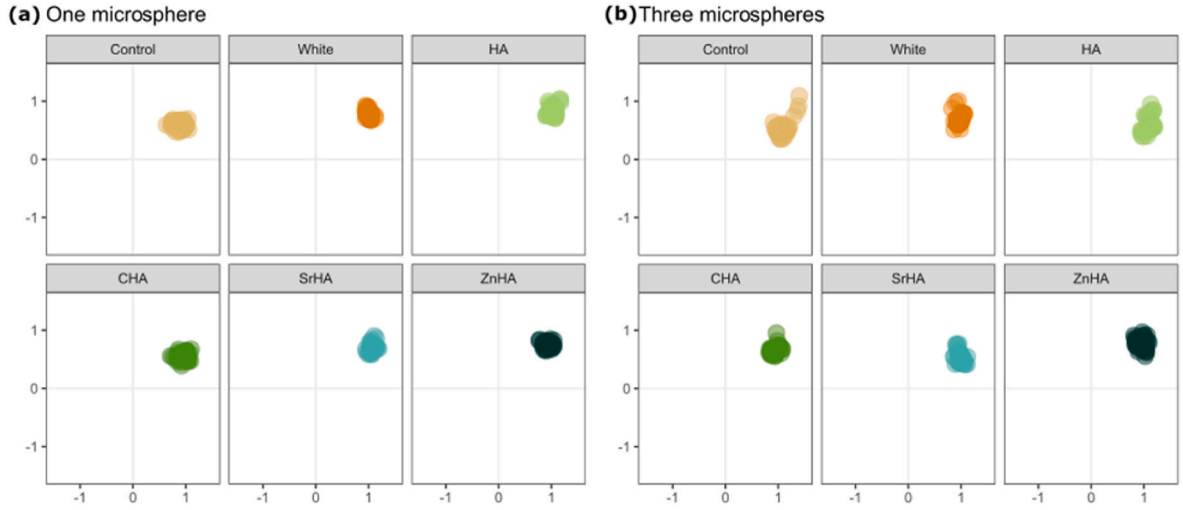

Fig. 6. The bubble plot shows the avoidance response for treatments with **(a)** one microsphere and **(b)** three microspheres of HA-based biomaterials. The X and Y coordinates indicate the position in the Cartesian plane where the individuals of each group spent most of their time in the test of avoidance response. LMM was performed and the Bonferroni post hoc test was applicating, when necessary.

calcium phosphate grafts brought new challenges in tissue regeneration due to the effects of resorption and the traffic of nanoparticles in cells and tissues. These issues are still little explored in the literature when calcium phosphates, especially HA, are used with ionic substitutions. The extensive use of these compounds justifies the investigation of their biosafety toxicity in a large quantity or number of models, including embryotoxicity.

The European Commission, the EU Reference Laboratory for Alternatives to Animal Testing (EURL ECVAM), the OECD, and other international agencies recommend the use of the Zebrafish Embryo Acute Toxicity Test (ZFET). It is accepted in scientific research and has been widely used in large companies as alternative model as it has great sensitivity and produces reliable data for the biosafety of new compounds. Thus, the zebrafish model is improving the prediction of human outcomes, a bridges the gap between in vitro and mammalian models as it allows analyzing complex data in a vertebrate, which would be impossible to explore in cellular models while fits the 3Rs of sustainability (Eimon and Rubinstein, 2009; Sobanska et al., 2018; von Hellfeld

et al., 2020). That is because zebrafish embryos and larvae have optical transparency, allowing real-time analysis of the chemical compound's interaction with the developing animal and higher experimental yield compared to vertebrate models.

The toxicological analysis of HA-based biomaterials in zebrafish embryos was studied by observing specific toxicological parameters up to 120 hpf. The first developmental stage (up to 24 hpf) is critical because several morphogenic movements occur during this period. Although the zebrafish embryos in the initial stages are high sensitivity, the tested biomaterials did not affect the development of the embryos. Even after 120 hpf exposure to HA, CHA, SrHA, and ZnHA microspheres with different patterns of crystallinity, porosity, nanoparticle size, and surface area, there was no mortality rate greater than 20%, indicating the non-embryotoxic feature of the tested biomaterials.

Several developmental delays were noted in zebrafish embryos after exposure to the DCA positive control, such as hatched embryos, effects on circulation, yolk sac edema, pericardial edema, malformed head and jaw, and deformed body shape. Besides being a positive control, the DCA shows that the zebrafish strain we used is sensitive to a compound known to be embryotoxic. This sensitivity should result in minimum mortality of 30% mortality at the 4 mg/L concentration. Regardless of the wild type strain, there may be differences in terms of sensitivity from one colony to another. Overall, there were no significant developmental differences in zebrafish embryos exposed to our biomaterials compared to the negative control.

In Xu et al. (2012), another study that evaluated the toxicological effect on the development of zebrafish embryos based on nanomaterials (nHA), ($nTiO_2$), and ($nSiO_2$), it was observed that none of the embryos died before hatching 3 dpf in the groups exposed to nHA and $nSiO_2$. Mortality data showed apparent toxicity at more than 100 mg/L $nTiO_2$. All embryos and larvae died at 400 mg/L $nTiO_2$ for 120 hpf of exposure, while only less than 30% died at 400 mg/L of $nSiO_2$. However, none of the embryos and larvae showed malformations and mortality in the 400 mg/L nHA groups (Xu et al., 2012).

In vitro studies with nano HA, CHA, SrHA, and ZnHA with different properties did not induce relevant cytotoxic, morphological, or pro-inflammatory effects, even at high doses, suggesting the biosafety of these biomaterials regardless of the physicochemical properties (Anjos et al., 2019; Calasans-Maia et al., 2015; Martinez-Zelaya et al., 2019; Mavropoulos et al., 2013). Despite the importance of in vitro studies, approaches in zebrafish embryos can provide greater acceptance in science, as they present greater sensitivity and better correspondence with humans than in vitro models.

A study of carbonated hydroxyapatite in zebrafish did not affect the decrease in survival and hatching rate, nor did it increase the malformation rate even at the highest concentrations (Pratama et al., 2021). However, in a toxicity study of needle-shaped (nHA-ND) and rod-shaped (nHA-RD) (nHA-RD) HA nanoparticles (nHA-RD), the authors analyzed the toxicological potential in vitro (catfish cells) and zebrafish embryos. Neither nHA-ND nor nHA-RD affects cell viability and thus, embryos showed complete development to larvae with normal morphology. However, approximately 75% of embryos incubated at the highest concentration of nHA-ND showed spinal deformation at 120hpf (Zhao et al., 2013).

However, when embryotoxicity tests did not show significant changes, morphological studies and mortality are limited data because neurological damage that may occur cannot be observed. Hence, additional endpoints must be included. Here, we expanded the embryo evaluation to obtain optomotor behavioral data in larvae, as these studies are often used to analyze the spatial response and detect visual-motor failures (LeFauve et al., 2021).

Although presenting a reduced cognitive repertoire compared to adults, zebrafish larvae show specific vision-oriented cognitive responses. This specificity of larvae visual orientation has led to the development of highly validated protocols to assess reflex responses and cognitive processing responses with high experimental throughput (Creton, 2009; Gonzalez et al., 2016; O'Neale et al., 2014; Richendrfer et al., 2012; Thorn et al., 2017).

The OMR (optomotor response) is a well-described reflex-orientating behavior in which zebrafish larvae move toward visual motion patterns (Fleisch and Neuhauss, 2006; Thorn et al., 2017). At both concentrations (1 and 3 microspheres), all experimental groups had a positive OMR. This result means that larvae were following the movements of the visual patterns. Furthermore, in this case, larvae exposed to one SrHA microsphere showed a better OMR than the White.

Another well-documented reflex behavior used to infer neurotoxicity is avoiding a bouncing ball. The avoidance behavior refers to a startle response triggered by visual stimuli when zebrafish larvae move away from dark areas, moving objects, or open spaces (Colwill and Creton, 2011). In the "bouncing ball" stimulus analysis, a total of 1440 larval positions per group were measured in those exposed by a microsphere and 1200 larval positions exposed to 3 microspheres, 80 images in two independent experiments (40-time points per experiment). In general, the larvae swam away from the bouncing ball and in the opposite direction to the aversive stimulus, and there was no significant difference to the negative control.

Previous studies recommend using zebrafish larvae with six or seven dpf, as there is reduced variability between subjects at these ages. In all our behavioral measures, including the activity of swimming away from the bouncing ball (escape or avoidance) and staying within a safe distance from the bouncing ball (passive avoidance), 6–7 dpf zebrafish showed proper behavioral responses. Although being a relatively simple method, it can be a trustworthy tool for behavioral analysis of cognitive and learning processes in zebrafish larvae (Creton, 2009; O'Neale et al., 2014; Richendrfer and Creton, 2018).

Although nothing came out of the toxicological and behavioral tests done here, molecular endpoint studies can often be helpful to elucidate the underlying pathways, as we cannot exclude the possibility of changes at the molecular level. Such effects do not affect morphology and behavior but can cause damage such as oxidative stress. Although oxidative stress is a natural process that occurs in cells, any imbalance may affect cell activities with consequences for the organism's development. The gene expression levels of sod1, sod2, cat, and gpx1 significantly affect antioxidative stress in cells and in vivo, so these genes are critical indicators to assess any change in the level of oxidative stress (Tao et al., 2022). However, the qPCR data presented here, focusing on four genes involved in oxidative stress protection, revealed a lack of these genes' alteration compared to the negative control, regardless of the biomaterial tested and conditions. Due to these data, our results were robust and indicated extremely low or absent toxicity of the compounds, allowing clinical application. Therefore, these findings support our hypothesis that functionalized HA-based biomaterials tested here do not have toxicological properties, being useful for medical devices.

5. Conclusion

The growing number of new HA-based functionalized biomaterials produced should be accompanied by an increase in studies to understand the biosafety of these compounds, employing a large number of models, including embryotoxicity. To date, this is the first study to illustrate the embryonic, developmental, and behavioral toxicity of ion-substituted HA graft exposure of zebrafish embryos to 4 to 120 hpf. In summary, our data suggest no toxicological effects of alginate microspheres graft containing nanoparticles of zinc-, strontium- and carbonate-substituted HA, nor changes in development and behavior.

Funding

This work was carried out with financial support from the Coordenação de Aperfeiçoamento de Pessoal de Nível Superior (CAPES) *finance code 001* and Conselho Nacional de Desenvolvimento Científico e

Tecnológico (CNPq)/Instituto Nacional de Ciência e Tecnologia em Medicina Regenerativa (INCT-Regenera, process n. 465,656/2014–5). The data from this research is part of the doctoral project of Augusto Monteiro de Souza in the Postgraduate Program in Biotechnology/RENORBIO, Federal University of Rio Grande do Norte, Brazil.

Credit author statement

Souza, AM: Conceptualization, Methodology, Data Curation, Investigation, Writing – original draft, Writing – review/editing. **Araujo-Silva, H:** Methodology, Data Curation, Writing – original draft, Writing – review/editing. **Luchiari, AC:** Conceptualization, Methodology, Data Curation, Writing – original draft, Writing – review/editing, Supervision. **Costa, AM:** Synthesis, characterization, and production of biomaterials Writing – original draft, Writing – review/editing. **Rossi, AL:** Transmission electron microscopy (TEM) analysis of nanoparticles, Writing – review/editing. **Rossi, AM:** Synthesis, characterization, and production of biomaterials, Writing – original draft, Writing – review/editing. **Granjeiro, JM:** Writing – review/editing. **Batistuzzo de Medeiros, SR:** Conceptualization, Methodology, Data Curation, Writing – original draft, Writing – review/editing, Supervision.All authors assisted in writing and reviewing and approving the final manuscript.

Declaration of competing interest

The authors declare that they have no known competing financial interests or personal relationships that could have appeared to influence the work reported in this paper.

Data availability

No data was used for the research described in the article.

Appendix A. Supplementary data

Supplementary data to this article can be found online at https://doi.org/10.1016/j.chemosphere.2022.137519.

References

Anjos, S. dos, Mavropoulos, E., Alves, G.G., Costa, A.M., de Alencar Hausen, M., Spiegel, C.N., Longuinho, M.M., Mir, M., Granjeiro, J.M., Rossi, A.M., 2019. Impact of crystallinity and crystal size of nanostructured carbonated hydroxyapatite on pre-osteoblast in vitro biocompatibility. J. Biomed. Mater. Res., Part A 107, 1965–1976. https://doi.org/10.1002/jbm.a.36709.

Bustin, S.A., Benes, V., Garson, J.A., Hellemans, J., Huggett, J., Kubista, M., Mueller, R., Nolan, T., Pfaffl, M.W., Shipley, G.L., Vandesompele, J., Wittwer, C.T., 2009. The MIQE Guidelines: Minimum Information for Publication of Quantitative Real-Time PCR Experiments. https://doi.org/10.1373/clinchem.2008.112797.

Calasans-Maia, M.D., Melo, B.R. de, Alves, A.T.N.N., Resende, R.F. de B., Louro, R.S., Sartoretto, S.C., Granjeiro, J.M., Alves, G.G., 2015. Cytocompatibility and biocompatibility of nanostructured carbonated hydroxyapatite spheres for bone repair. J. Appl. Oral Sci. 23, 599–608. https://doi.org/10.1590/1678-775720150122.

Cao, J., Lian, R., Jiang, X., 2020. Magnesium and fluoride doped hydroxyapatite coatings grown by pulsed laser deposition for promoting titanium implant cytocompatibility. Appl. Surf. Sci. 515, 146069 https://doi.org/10.1016/j.apsusc.2020.146069.

Coelho, F., Cavicchioli, M., Specian, S.S., Scarel-Caminaga, R.M., Penteado, L. de A., de Medeiros, A.I., de Lima Ribeiro, S.J., de Oliveira Capote, T.S., 2019. Bacterial cellulose membrane functionalized with hydroxiapatite and anti-bone morphogenetic protein 2: a promising material for bone regeneration. PLoS One 14. https://doi.org/10.1371/journal.pone.0221286.

Colwill, R.M., Creton, R., 2011. Locomotor behaviors in zebrafish (Danio rerio) larvae. Behav. Process. 86, 222–229. https://doi.org/10.1016/j.beproc.2010.12.003.

Creton, R., 2009. Automated analysis of behavior in zebrafish larvae. Behav. Brain Res. 203, 127–136. https://doi.org/10.1016/j.bbr.2009.04.030.

Dewi, A.H., Ana, I.D., 2018. The use of hydroxyapatite bone substitute grafting for alveolar ridge preservation, sinus augmentation, and periodontal bone defect: a systematic review. Heliyon 4, e00884. https://doi.org/10.1016/j.heliyon.2018.e00884.

Eimon, P.M., Rubinstein, A.L., 2009. The use of in vivo zebrafish assays in drug toxicity screening. Expet Opin. Drug Metabol. Toxicol. 5, 393–401. https://doi.org/10.1517/17425250902882128.

Ferdous, Z., Nemmar, A., 2020. Health impact of silver nanoparticles: a review of the biodistribution and toxicity following various routes of exposure. Int. J. Mol. Sci. 21, 1–31. https://doi.org/10.3390/ijms21072375.

Fleisch, V.C., Neuhauss, S.C.F., 2006. Visual behavior in zebrafish. Zebrafish 3, 191–201. https://doi.org/10.1089/zeb.2006.3.191.

Ghorbani, F.M., Kaffashi, B., Shokrollahi, P., Seyedjafari, E., Ardeshirylajimi, A., 2015. PCL/chitosan/Zn-doped nHA electrospun nanocomposite scaffold promotes adipose derived stem cells adhesion and proliferation. Carbohydr. Polym. 118, 133–142. https://doi.org/10.1016/j.carbpol.2014.10.071.

Gonzalez, S.T., Remick, D., Creton, R., Colwill, R.M., 2016. Effects of embryonic exposure to polychlorinated biphenyls (PCBs) on anxiety-related behaviors in larval zebrafish. Neurotoxicology 53, 93–101. https://doi.org/10.1016/j.neuro.2015.12.018.

Kassambara, A., 2020a. Rstatix: Pipe-Friendly Framework for Basic Statistical Tests. R package version 0.5.0.999. R Packag. version 0.6.0. https://rpkgs.datanovia.com/rstatix/.

Kassambara, A., 2020b. Package ' Ggpubr ' [WWW Document]. [Accessed Apr. 2020]. Available from:; https//rpkgs.datanovia.com/ggpubr/BugReports.

LeFauve, M.K., Rowe, C.J., Crowley-Perry, M., Wiegand, J.L., Shapiro, A.G., Connaughton, V.P., 2021. Using a variant of the optomotor response as a visual defect detection assay in zebrafish. J. Biol. Methods 8, e144. https://doi.org/10.14440/jbm.2021.341.

Lenth, R., Lenth, M.R., 2018. Package 'lsmeans.'. Am. Statistician 34, 216–221.

Lin, Sijie, Zhao, Y., Nel, A.E., Lin, Shuo, 2013. Zebrafish: an in vivo model for nano EHS studies. Small 9, 1608–1618. https://doi.org/10.1002/smll.201202115.

Martinez-Zelaya, V.R., Zarranz, L., Herrera, E.Z., Alves, A.T., Uzeda, M.J., Mavropoulos, E., Rossi, A.L., Mello, A., Granjeiro, J.M., Calasans-Maia, M.D., Rossi, A.M., 2019. In vitro and in vivo evaluations of nanocrystalline Zn-doped carbonated hydroxyapatite/alginate microspheres: zinc and calcium bioavailability and bone regeneration. Int. J. Nanomed. 14, 3471–3490. https://doi.org/10.2147/IJN.S197157.

Mavropoulos, E., Hausen, M., Costa, A.M., Alves, G., Mello, A., Ospina, C.A., Mir, M., Granjeiro, J.M., Rossi, A.M., 2013. The impact of the RGD peptide on osteoblast adhesion and spreading on zinc-substituted hydroxyapatite surface. J. Mater. Sci. Mater. Med. 24, 1271–1283. https://doi.org/10.1007/s10856-013-4851-3.

Melchior, K., Saska, S., Coelho, F., Scarel-Caminaga, R.M., de Oliveira Capote, T.S., 2018. BONEFILL (R) block as alternative for bone substitute: a toxicological evaluation. Brazil. J. Pharm. Sci. 54 https://doi.org/10.1590/s2175-97902018000217438.

Melchor-Martínez, E.M., Torres Castillo, N.E., Macias-Garbett, R., Lucero-Saucedo, S.L., Parra-Saldívar, R., Sosa-Hernández, J.E., 2021. Modern world applications for nano-bio materials: tissue engineering and COVID-19. Front. Bioeng. Biotechnol. 9, 1–16. https://doi.org/10.3389/fbioe.2021.597958.

Mohan, N., Palangadan, R., Fernandez, F.B., Varma, H., 2018. Preparation of hydroxyapatite porous scaffold from a 'coral-like' synthetic inorganic precursor for use as a bone substitute and a drug delivery vehicle. Mater. Sci. Eng. C 92, 329–337. https://doi.org/10.1016/j.msec.2018.06.064.

Morscher, E.W., Surgery, O., Müller, M.E., Hefti, A., Aebi, U., 1998. Severe osteolysis after third-body wear due to hydroxyapatite particles from acetabular cup coating. J. Bone Jt. Surg [Br] 80, 80–267.

Mosa, I.F., Abd, H.H., Abuzreda, A., Assaf, N., Yousif, A.B., 2020. Bio-evaluation of the role of chitosan and curcumin nanoparticles in ameliorating genotoxicity and inflammatory responses in rats' gastric tissue followed hydroxyapatite nanoparticles' oral uptake. Toxicol. Res. 9, 493–508. https://doi.org/10.1093/toxres/tfaa054.

O'Neale, A., Ellis, J., Creton, R., Colwill, R.M., 2014. Single stimulus learning in zebrafish larvae. Neurobiol. Learn. Mem. 108, 145–154. https://doi.org/10.1016/j.nlm.2013.08.016.

Pratama, S.F., Ana, I.D., Retnoaji, B., 2021. The effect of carbonate hydroxyapatite (CHA) dental implant material on the early development of zebrafish embryos (Danio rerio). In: Proceedings of the 3rd KOBI Congress. International and National Conferences, pp. 307–312. https://doi.org/10.2991/absr.k.210621.052. KOBICINC 2020).

Ratnayake, J.T.B., Mucalo, M., Dias, G.J., 2016. Substituted hydroxyapatites for bone regeneration: a review of current trends. J. Biomed. Mater. Res. B Appl. Biomater. 105, 1285–1299. https://doi.org/10.1002/jbm.b.33651.

Remya, N.S., Syama, S., Sabareeswaran, A., Mohanan, P.V., 2017. Investigation of chronic toxicity of hydroxyapatite nanoparticles administered orally for one year in wistar rats. Mater. Sci. Eng. C 76, 518–527. https://doi.org/10.1016/j.msec.2017.03.076.

Richendrfer, H., Creton, R., 2018. Cluster analysis profiling of behaviors in zebrafish larvae treated with antidepressants and pesticides. Neurotoxicol. Teratol. 69, 54–62. https://doi.org/10.1016/j.ntt.2017.10.009.

Richendrfer, H., Pelkowski, S.D., Colwill, R.M., Créton, R., 2012. Developmental sub-chronic exposure to chlorpyrifos reduces anxiety-related behavior in zebrafish larvae. Neurotoxicol. Teratol. 34, 458–465. https://doi.org/10.1016/j.ntt.2012.04.010.

Sari, M., Hening, P., Chotimah Ana, I.D., Yusuf, Y., 2021. Bioceramic hydroxyapatite-based scaffold with a porous structure using honeycomb as a natural polymeric Porogen for bone tissue engineering. Biomater. Res. 25, 2. https://doi.org/10.1186/s40824-021-00203-z.

Sobanska, M., Scholz, S., Nyman, A.-M., Cesnaitis, R., Gutierrez Alonso, S., Klüver, N., Kühne, R., Tyle, H., de Knecht, J., Dang, Z., Lundbergh, I., Carlon, C., De Coen, W., 2018. Applicability of the fish embryo acute toxicity (FET) test (OECD 236) in the regulatory context of Registration, Evaluation, Authorisation, and Restriction of Chemicals (REACH). Environ. Toxicol. Chem. 37, 657–670. https://doi.org/10.1002/etc.4055.

Subramaniam, S., Fang, Y.-H., Sivasubramanian, S., Lin, F.-H., Lin, C., 2016. Hydroxyapatite-calcium sulfate-hyaluronic acid composite encapsulated with collagenase as bone substitute for alveolar bone regeneration. Biomaterials 74, 99–108. https://doi.org/10.1016/j.biomaterials.2015.09.044.

Tao, Z.-S., Wang, H.-S., Li, T.-L., Wei, S., 2022. Silibinin-modified Hydroxyapatite coating promotes the osseointegration of titanium rods by activation SIRT1/SOD2 signaling pathway in diabetic rats. J. Mater. Sci. Mater. Med. 33, 62. https://doi.org/10.1007/s10856-022-06684-1.

Terra, J., Dourado, E.R., Eon, J.G., Ellis, D.E., Gonzalez, G., Rossi, A.M., 2009. The structure of strontium-doped hydroxyapatite: an experimental and theoretical study. Phys. Chem. Chem. Phys. 11, 568–577. https://doi.org/10.1039/b802841a.

Terra, J., Jiang, M., Ellis, D.E., 2002. Characterization of electronic structure and bonding in hydroxyapatite: Zn substitution for Ca. Philos. Mag. A Phys. Condens. Matter, Struct. Defects Mech. Prop. 82, 2357–2377. https://doi.org/10.1080/01418610208235744.

Thorn, R.J., Clift, D.E., Ojo, O., Colwill, R.M., Creton, R., 2017. The loss and recovery of vertebrate vision examined in microplates. PLoS One 12, 1–17. https://doi.org/10.1371/journal.pone.0183414.

Turkez, H., Yousef, M.I., Sönmez, E., Togar, B., Bakan, F., Sozio, P., Stefano, A. Di, 2014. Evaluation of cytotoxic, oxidative stress and genotoxic responses of hydroxyapatite nanoparticles on human blood cells. J. Appl. Toxicol. 34, 373–379. https://doi.org/10.1002/jat.2958.

Venkateswarlu, K., Sandhyarani, M., Nellaippan, T.A., Rameshbabu, N., 2014. Estimation of crystallite size, lattice strain and dislocation density of nanocrystalline carbonate substituted hydroxyapatite by X-ray peak variance analysis. Procedia Mater. Sci. 5, 212–221. https://doi.org/10.1016/j.mspro.2014.07.260.

von Hellfeld, R., Brotzmann, K., Baumann, L., Strecker, R., Braunbeck, T., 2020. Adverse effects in the fish embryo acute toxicity (FET) test: a catalogue of unspecific morphological changes versus more specific effects in zebrafish (Danio rerio) embryos. Environ. Sci. Eur. 32, 122. https://doi.org/10.1186/s12302-020-00398-3.

Wang, P., Li, C., Gong, H., Jiang, X., Wang, H., Li, K., 2010. Effects of synthesis conditions on the morphology of hydroxyapatite nanoparticles produced by wet chemical process. Powder Technol. 203, 315–321. https://doi.org/10.1016/j.powtec.2010.05.023.

Wang, P., Zhao, L., Liu, J., Weir, M.D., Zhou, X., Xu, H.H.K., 2014. Bone tissue engineering via nanostructured calcium phosphate biomaterials and stem cells. Bone Res. 2, 14017 https://doi.org/10.1038/boneres.2014.17.

Wickham, H., Averick, M., Bryan, J., Chang, W., McGowan, L., François, R., Grolemund, G., Hayes, A., Henry, L., Hester, J., Kuhn, M., Pedersen, T., Miller, E., Bache, S., Müller, K., Ooms, J., Robinson, D., Seidel, D., Spinu, V., Takahashi, K., Vaughan, D., Wilke, C., Woo, K., Yutani, H., 2019. Welcome to the tidyverse. J. Open Source Softw. 4, 1686. https://doi.org/10.21105/joss.01686.

Xu, Z., Zhang, Y.-L., Song, C., Wu, L.-L., Gao, H.-W., 2012. Interactions of hydroxyapatite with proteins and its toxicological effect to zebrafish embryos development. PLoS One 7, e32818. https://doi.org/10.1371/journal.pone.0032818.

Zhao, X., Ong, K.J., Ede, J.D., Stafford, J.L., Ng, K.W., Goss, G.G., Loo, S.C.J., 2013. Evaluating the toxicity of hydroxyapatite nanoparticles in catfish cells and zebrafish embryos. Small 9, 1734–1741. https://doi.org/10.1002/smll.201200639.